CD38/ADP-Ribosyl Cyclase: A New Role in the Regulation of Osteoclastic Bone Resorption

Li Sun,* Olugbenga A. Adebanjo,* Baljit S. Moonga,* Susanne Corisdeo,‡ Hindupur K. Anandatheerthavarada,§ Gopa Biswas,§ Toshiya Arakawa,¶ Yoshiyuki Hakeda,¶ Antoliy Koval,* Bali Sodam,* Peter J.R. Bevis,* A. James Moser,* F. Anthony Lai,‖ Solomon Epstein,* Bruce R. Troen,‡ Masayoshi Kumegawa,¶ and Mone Zaidi*

*Center for Osteoporosis and Skeletal Aging, Department of Medicine, Medical College of Pennsylvania and Veterans Affairs Medical Center, Philadelphia, Pennsylvania 19104; ‡Lankanau Medical Research Center, Merion, Pennsylvania 19066; §School of Veterinary Medicine, University of Pennsylvania, Philadelphia, Pennsylvania 19104; ‖Department of Medicine, University of Cardiff, Cardiff, United Kingdom; and ¶Mekai University, Saitama, Japan

Abstract. The multifunctional ADP-ribosyl cyclase, CD38, catalyzes the cyclization of NAD^+ to cyclic ADP-ribose (cADPr). The latter gates Ca^{2+} release through microsomal membrane-resident ryanodine receptors (RyRs). We first cloned and sequenced full-length CD38 cDNA from a rabbit osteoclast cDNA library. The predicted amino acid sequence displayed 59, 59, and 50% similarity, respectively, to the mouse, rat, and human CD38. In situ RT-PCR revealed intense cytoplasmic staining of osteoclasts, confirming CD38 mRNA expression. Both confocal microscopy and Western blotting confirmed the plasma membrane localization of the CD38 protein. The ADP-ribosyl cyclase activity of osteoclastic CD38 was next demonstrated by its ability to cyclize the NAD^+ surrogate, NGD^+, to its fluorescent derivative cGDP-ribose. We then examined the effects of CD38 on osteoclast function. CD38 activation by an agonist antibody (A10) in the presence of substrate (NAD^+) triggered a cytosolic Ca^{2+} signal. Both ryanodine receptor modulators, ryanodine, and caffeine, markedly attenuated this cytosolic Ca^{2+} change. Furthermore, the anti-CD38 agonist antibody expectedly inhibited bone resorption in the pit assay and elevated interleukin-6 (IL-6) secretion. IL-6, in turn, enhanced CD38 mRNA expression. Taken together, the results provide compelling evidence for a new role for CD38/ADP-ribosyl cyclase in the control of bone resorption, most likely exerted via cADPr.

Key words: Ca^{2+} channel • ryanodine receptor • bone resorption • cADPr • osteoporosis

CD38/ADP-ribosyl cyclase is a key cellular enzyme that catalyses the cyclization of the intermediary metabolite, nicotinamide adenine dinucleotide (NAD^+), to the putative second messenger, cyclic ADP-ribose (cADPr)[1]. The latter activates Ca^{2+} release from RyR-gated Ca^{2+} stores (Lee et al., 1994; DeFlora et al., 1998). CD38 is widely distributed in hemopoietic cells, including B and T lymphocytes, thymocytes, plasma cells, macrophages, and erythrocytes, as well as in kidney, cardiac, pancreatic, brain, spleen, lung, and liver cells (Malavasi et al., 1992; Lee et al., 1996, 1997; Shubinski and Schlesinger, 1997; Fernandez et al., 1998). Structurally, CD38 is a monomeric, 46-kD, type II glycoprotein with a short NH_2-terminal cytoplasmic tail, a single membrane-spanning region, and a long extracellular COOH-terminal catalytic domain (Lee et al., 1994). The cDNAs encoding human, mouse, and rat CD38 have been cloned. The deduced murine and rat CD38 sequences display ~75% homology with the human sequence (Harada et al., 1993; Mehta et al., 1996; Ferrero and Malavasi, 1997).

Apart from being an ADP-ribosyl cyclase, CD38 can function as a NAD^+ glycohydrolase and an ADPr hydrolase (Lee et al., 1994; Berthelier et al., 1998). Intracellularly generated cADPr is thought to play the role of a cellular second messenger (for review, see Lee, 1996; Guse et al., 1999). It is also considered a receptor for CD31 in B and T lymphocytes (Deaglio et al., 1998; Horenstein et al.,

L. Sun and O.A. Adebanjo contributed equally to this paper.

Address correspondence to Mone Zaidi, Division of Endocrinology, Box 1055, Mount Sinai School of Medicine, 1 Gustave Levy Place, New York, NY 10029. Tel.: (212) 241-8797. E-mail: mone.zaidi@smtplink.mssm.edu

1. *Abbreviations used in this paper:* BCIP, 5-bromo-4-chloro-3-indoyl-phosphate; cADPr, cyclic ADP-ribose; IL-6, interleukin 6; NBT, 4-nitro-blue tetrazolium chloride; RyRs, ryanodine receptors; TRAP, tartrate-resistant acid phosphatase.

1998). There is further evidence that plasma membrane CD38 internalizes upon binding to monoclonal antibodies (Funaro et al., 1998) and NAD^+ (Zocchi et al., 1999). The latter would yield intracellular cADPr that could potentially activate microsomal membrane RyRs (Zocchi et al., 1999). Also of note is that NAD^+, being an intermediary metabolite, could couple a cell's metabolic activity to its Ca^{2+} level via the CD38/cADPr pathway.

It is now well established that the osteoclast, a cell that is unique in its ability to resorb bone, can monitor changes in its ambient Ca^{2+} level by means of a Ca^{2+} sensor (Malgaroli et al., 1989; Zaidi et al., 1989, 1993; Moonga et al., 1990). A high extracellular Ca^{2+}, through a rise in cytosolic Ca^{2+}, triggers dramatic osteoclast retraction, and in the longer term, a marked inhibition of acid secretion, enzyme release, and bone resorption (Malgaroli et al., 1989; Zaidi et al., 1989; Datta et al., 1990; Miyauchi et al., 1990; Moonga et al., 1990). We believe that a type 2 ryanodine receptor (RyR-2), positioned uniquely in the osteoclast plasma membrane, functions as a Ca^{2+} channel, and possibly a Ca^{2+} sensor (Zaidi et al., 1995). Ordinarily, RyRs are located in microsomal membranes and gate Ca^{2+} release in response to both Ca^{2+} and cADPr.

Ca^{2+} sensing in the osteoclast is regulated by several systemic and local factors, namely calcitonin, interleukin-6 (IL-6), ambient pH, and membrane potential (Zaidi et al., 1996; Adebanjo et al., 1994, 1998; Shankar et al., 1995). We have shown recently that IL-6 attenuates the inhibitory effect of Ca^{2+} on the osteoclast (Adebanjo et al., 1998). Ca^{2+} in turn enhances IL-6 secretion, possibly as part of a feedback signal to maintain resorption even in the face of a rising Ca^{2+} (Adebanjo et al., 1998). Of note is that, during resorption, an osteoclast's metabolic requirements and, hence, its NAD^+ levels, are likely to increase dramatically because of active proton and enzyme secretion.

This study examines whether CD38/ADP ribosyl cyclase has a new role in the regulation of osteoclastic bone resorption. We first report the cloning and sequencing of cDNA encoding a novel CD38 homologue. Furthermore, we demonstrate that CD38 mRNA is expressed in the osteoclast; that immunoreactive CD38 is localized to the cell's plasma membrane; that the enzyme displays ADP ribosyl cyclase activity in the $NGD^+ \rightarrow$cGDPr assay; that, when activated, CD38 triggers a cytosolic Ca^{2+} signal through ryanodine receptor activation; and that the CD38-induced Ca^{2+} signal is associated with resorption inhibition and IL-6 release. We postulate that NAD^+ couples an osteoclast's metabolic activity to its resorptive function using CD38 and cADPr as the sensor and signal, respectively.

Materials and Methods

Osteoclast Cultures

Long bones obtained from neonatal Wistar rats killed by decapitation were curetted into Hepes-buffered Medium 199 containing Hank's salts (GIBCO-BRL) and heat-inactivated fetal bovine serum (FBS, 5% vol/vol; Sigma Chemical Co.) (M199-H). The resulting suspension was dispersed onto devitalized cortical bone slices or 22-mm, 0-grade, glass coverslips (Libro/ICN). Osteoclasts attached to the respective substrate within 15 min (37°C) and contaminating cells were removed by gentle rinsing. Osteoclasts were identified readily by their large size, multinuclearity, complex morphology, densely ruffling edges, and response to calcitonin (Zaidi et al., 1992).

Purified rabbit osteoclasts were prepared by the method of Kakudo et al. (1996) from unfractionated bone cells obtained according to the procedure described by Tezuka et al. (1992). In brief, cell suspensions obtained from minced long bones of 10-d-old rabbits (Japan White; Saitama Experimental Animal Supply Co.) were agitated by vortexing and plated in 10-cm tissue culture dishes (Becton Dickinson) coated with 24% collagen gel (Nitta Gelatin Co.). After a 3-h incubation, adherent non-osteoclasts were removed from the collagen gel by sequential treatment with pronase E (0.001% wt/vol) and collagenase (0.01%, wt/vol; Wako Pure Chemical Industries). The remaining osteoclasts were then collected by 0.1% (wt/vol) collagenase solution treatment and replated. When these cell suspensions were seeded onto tissue culture dishes, osteoclasts attached and spread out. The purity of the osteoclast preparation was judged before membrane isolation by staining for an osteoclast-specific marker, tartrate-resistant acid phosphatase (TRAP) using a leukocyte acid phosphatase kit (Sigma). In line with previous experiments of Kameda et al. (1997), we found that the purity of TRAP-positive multinucleated cells (>3 nuclei) was >99%. These cells have been shown to resorb bone and express specific osteoclast markers, cathepsin K, and calcitonin receptors (Takeda et al., 1992; Kameda et al., 1997, 1998).

Isolation and Sequencing of CD38 cDNA Clone from a Rabbit Osteoclast cDNA Library

A rabbit osteoclast cDNA library containing 1×10^{10} independent clones was used for PCR amplification (Tezuka et al., 1992; Kameda et al., 1998). Two oligonucleotide primers were designed from the known rat CD38 cDNA sequence (these data are available from GenBank/EMBL/DDBJ under accession number D29646): forward primer, 5′-CCTGTTGCTGTGTTCTGGA-3′ (569–588), and reverse primer, 5′-GGTCGGTAGTTATCCTGG C-3′ (861–843) (GIBCO-BRL). The coding region of rabbit CD38 cDNA fragment was then amplified by PCR. In brief, the standard reaction mixture (50 μl) contained: 0.1 μl of rabbit osteoclast cDNA library, 1 μl of each oligonucleotide (50 μl), and 1 μl (5 U) of AmpliTaq (Promega Corp.). The GeneAmp PCR System 2400 (Perkin Elmer) was programmed as follows: a 5-min cycle at 95°C, then 40, 1-min cycles at 95, 55, and 72°C. The PCR products were separated by agarose gel electrophoresis. A ~300-bp DNA fragment was isolated from excised gel slices using a QIAquick Gel Extraction Kit (QIAGEN Inc.) and ligated into EcoRV-cut pBluescript II SK (+/−) vector (Stratagene Ltd.) to produce the plasmid, pBS-CD38, which was then transformed into competent DH5α cells. 293 bp of pBS-CD38 insert was confirmed through the DNA Sequencing Facility at the University of Pennsylvania.

To obtain the full-length CD38 cDNA, the 293-bp CD38 coding region DNA fragment was used as probe to screen our osteoclast cDNA library (by a method described by Sambrook, 1989). For this, the probe was labeled with α-[^{32}P]CTP (3,000 Ci/mmol) (NEN™ Life Science Products Inc.) using the *Red*prime Random Prime Labeling Kit (Amersham Pharmacia Biotech Inc.). Duplicate filters, which covered 1×10^7 independent clones, were then hybridized overnight at 42°C with prehybridization solution (50% formamide, 6× SSC, 5× Denhardt's, 0.5% SDS, 0.1 mg/ml denatured fragmented salmon sperm DNA) to which a labeled probe was added 3 h later. After a high-strigency wash at 68°C for 1 h, the filters were exposed to x-ray film with intensifying screens for 20 h at −70°C. Positive recombinant plaques were purified from phage plate lysates according to the Lambda ZAP II library's instruction manual (Stratagene). The DNA clones were confirmed by PstI-KpnI restriction analysis and direct nucleotide sequencing.

CD38 mRNA Expression in Single Osteoclasts Revealed by In Situ RT-PCR Cytoimaging

We and others have recently applied in situ RT-PCR cytoimaging successfully to study IL-6 and IL-6 receptor expression in osteoblasts, osteoclasts, and bone marrow stromal cells (Lin et al., 1997; Adebanjo et al., 1998). We now utilize this technology to examine CD38 expression in mature rat osteoclasts (primer sequences, as above). As a positive control, we also examined the expression of a housekeeping gene (glyceraldehyde 3-phosphate dehydrogenase, GADPH, data available from GenBank/EMBL/DDBJ under accession number M32599) and an osteoclast-specific gene (cathepsin K, accession number AF010306). Their primer sequences were: GAPDH, forward: 5′-TGAAGGTCGGTGTGAACGGATTTGGC-3′

(51–76), reverse: 5′-CATGTAGGCCATGAGGTCCACCAC-3′ (1033–1010); cathepsin K, forward: 5′-CCCAGACTCCATCGACTATCG-3′ (345–365), reverse: 5′-CTGTACCCTCTGCATTTAGCTGCC-3′ (674–651).

Osteoclasts were incubated on glass coverslips (22 mm, 0 grade) in Medium 199 with Earle's salts (6.6 mM Na_2CO_3, M199-E) for 6 h (37°C, 5% humidified CO_2, pH 7.4). In separate experiments, the cells were incubated with either vehicle or IL-6 (10 ng/liter or 10 μg/liter). The cultures were washed with M199-E, fixed with paraformaldehyde (4% vol/vol) in phosphate-buffered saline (PBS) (20 min, 4°C), and washed twice with cold PBS. The fixed cells were treated with 0.2 N-HCl (20 min, 20°C), washed with DEPC-water (Sigma Chemical Co.), and treated with proteinase-K (5 mg/liter in 10 mM Tris-HCl, pH 8, 15 min, 37°C) and cold paraformaldehyde (4% vol/vol, 30 min, 4°C). Before being air-dried, the cells were dehydrated by sequential 1-min immersions in graded aqueous ethanol solutions, 70, 80, 90, and 100% (vol/vol). They were then incubated overnight (37°C) with RNase-free DNase I (1,500 units/ml; Boehringer Mannheim) to remove genomic DNA. The DNase I was finally washed out with DEPC-water and inactivated by heating (90°C, 10 min).

First-strand cDNA was synthesized by incubating cultures with RT mixture (50 μl) comprising 1 mM dNTP, 0.01 M DTT, 400 nM reverse primer (above), DEPC-water, and 14 U/ml Superscript RT II (GIBCO-BRL) (42°C, 60 min). An AmpliCover disc was used to cover each sample. The samples were then treated separately with PCR mixture (50 μl) comprising 0.2 mM dNTP, PCR buffer, 2.5 mM $MgCl_2$, 0.1 U/μl Taq polymerase, 400 nM forward and reverse primers, 10 μM digoxigenin (DIG)-labeled-11-dUTP (Boehringer Mannheim), and DEPC-water. Each sample was then covered gently with an AmpliCover disc ensuring the absence of air bubbles. The GeneAmp In situ PCR System 1000 (Perkin Elmer) was programmed as follows. A 4-min soak at 94°C was followed by 40 cycles of: 94°C for 1 min, 55°C for 2 min, and 72°C for 3 min.

Incorporated DIG-11-dUTP in the PCR product was detected by an alkaline phosphatase (AP)-conjugated anti-DIG antiserum and AP substrates, 4-nitroblue tetrazolium chloride (NBT) and 5-bromo-4-chloro-3-indoyl-phosphate (BCIP) using a DIG Nucleic Acid Detection Kit (Boehringer Mannheim) per manufacturer's protocol. Negative controls, in which primers were omitted, were run in parallel. Messenger RNA expressing cells stained dark purplish brown, while negative controls did not stain.

We then performed an analysis of the staining intensity using a blinded observer. Osteoclasts were scored on a scale from 0 to 4 (no staining to intense staining, see legend to Fig. 4). The results from three experiments were plotted as a frequency histogram. This allowed us to determine the proportion of cells that lay in a certain intensity range. A similar analysis has been used by us previously (Adebanjo et al., 1998) to demonstrate the effects of Ca^{2+} on IL-6 and IL-6 receptor mRNA expression. Notably, GAPDH, a housekeeping gene, was used to control for the effects of IL-6 on CD38 expression. Also note, that, as previously, the few retracted osteoclasts were discarded from the analysis to prevent a biased intensity assessment.

Antibodies

Dr. F. Malavasi (Torino, Italy) kindly provided the monoclonal anti-CD38 antibody, A10. A10 was raised by immunizing mice with Burkitt's lymphoma Daudi cells (Malavasi et al., 1984, 1985). The antibody recognizes a 46-kD CD38 molecule on T and B lymphocytes also enhancing their activation and proliferation (hence the term, agonist) (Funaro et al., 1990). An antagonist antibody (Sigma Chemical Co.) was also used to establish specificity for CD38 detection in the ADP ribosyl cyclase assay. The control anti-ryanodine receptor antibody, Ab^{34}, was raised against a cytosolic calmodulin-binding RyR epitope. Therefore, it does not stain nonpermeabilized osteoclasts (Zaidi et al., 1995).

Immunocytochemistry and Confocal Microscopic Analysis

Osteoclasts were incubated with normal goat serum (in 10 mM PBS, 1:10, pH, 7.4, 15 min) in multiwell dishes and washed with HBSS (GIBCO-BRL). The cells were either incubated without antibody, or with nonimmune mouse IgG, Ab^{34} (anti-RyR antibody) (all controls), or A10 (anti-CD38 antibody) (in M199-H, 1:100). In the same experiment, CD38-negative fibroblasts were also incubated with the same antibodies. The coverslips were rinsed gently with HBSS, drained, reincubated with goat anti–mouse FITC (Sigma Chemical Co.; 1:100, in HBSS, 60 min), washed gently, and finally, drained. The number of fluorescent osteoclasts was first determined in a laser confocal scanning microscope, at λ_{ex} = 495 nm and λ_{em} = 525 nm (Leica Inc.). To localize staining to the osteoclast membrane, 1-μm-thick optical sections were obtained in the cell's coronal plane in selected experiments. Finally, trypan blue (1 mM, 961 Da; Sigma Chemical Co.) was applied to exclude membrane damage that could allow antibody access into the cell.

Membrane Isolation and Western Blot Analysis

For isolation of plasma membranes, cells were first scraped and homogenized in TKM solution (50 mM Tris-HCl, pH 7.5, 25 mM KCl and 5 mM $MgCl_2$) supplemented with 0.25 mM sucrose. The homogenate was centrifuged (3,000 *g*, 10 min), the pellet resuspended in sucrose (70% wt/vol), and then rehomogenized (12 strokes) with a glass/Teflon homogenizer. The sucrose solution was then layered as follows: the homogenate was overlaid with 12 ml of 48% (wt/vol) sucrose, followed by 6 ml of 42% (wt/vol) sucrose. This was then centrifuged at 27,700 rpm for 70 min in a SW-28 swinging bucket rotor. The plasma membrane fraction banding at the interface of 70%/48% sucrose was collected and suspended in 70% (wt/vol) sucrose solution. The entire process was repeated twice to purify the plasma membranes.

SDS-PAGE was performed using 12% separating and 4% stacking polyacrylamide gels using a minigel system (BioRad Laboratories). Plasma membranes prepared from osteoclasts and osteoblasts (30 μg protein) were heated for 5 min at 95°C in Laemelli's sample buffer (2% SDS, 2% β-mercaptoethanol, 10% vol/vol glycerol and 50 mg/liter bromophenol blue in 0.1 M Tris-HCl buffer, pH 6.8). Electrophoresis was performed at 20 mAmps per gel. The proteins thus resolved were stained with Coomassie Brilliant Blue (Sigma Chemical Co.) or transferred electrophoretically onto OPTITRAN-supported nitrocellulose membrane (Schleicher and Schuell) at 15°C for 1 h at 100 volts. The membranes were blocked with Tween 20 (0.3% vol/vol) in PBS at 20°C and incubated with the anti-CD38 antibody (1:3,000) (Sigma Chemical Co.). After rinsing, the blot was incubated for 1 h with HRP-conjugated anti–mouse antibody. The blot was developed using Pierce SuperSignal Ultra Chemiluminescence Kit, per manufacturer's instructions.

ADP-Ribosyl Cyclase ($NGD^+ \rightarrow$cGDPr) Assay

ADP-ribosyl cyclase activity was measured in osteoclast plasma membranes isolated as above. We measured the cyclization of the NAD^+ surrogate, NGD^+, to its fluorescent derivative, cGDPr. Plasma membranes (25 μg) were incubated, for 20 min at 37°C, in 20 mM Tris-HCl (pH 7.4) with 100 μM NGD^+. The reaction was stopped with 5 μl of 100% (vol/vol) trichloroacetic acid. Fluorescence in the supernatant was measured using a high-sensitivity spectrofluorometer (λ_{ex} = 300 nm; λ_{em} = 410 nm). The amount of cGDPr formed was plotted as mean ± SD in nmol/ml/mg protein. To establish specificity of the assay, we incubated membranes in with anti-CD38 antibody (1:1,000; Sigma Chemical Co.) and NAD^+ (400 μM). Mouse IgG5 was used as control.

Measurement of Cytosolic Ca^{2+} in Single Osteoclasts

Glass coverslips containing freshly isolated osteoclasts were incubated in serum-free medium (30 min, 37°C) with 10 μM fura 2/AM (Molecular Probes), then washed in M199-H and transferred to a Perspex bath positioned on the microspectrofluorometer stage. The latter was previously constructed from an inverted microscope (Diaphot; Nikon) (Shankar et al., 1992). Prewarmed test solutions of the anti-CD38 antibodies (A10, agonist and antagonist; Sigma Chemical Co.) (1:500), NAD^+ (0.5, 1, or 10 mM), ryanodine (5 μM), caffeine (250 μM and 1 mM), or thapsigargin (4 μM) were applied in various protocols, as described in Results. The cells were exposed alternatively to excitation λ^s of 340 or 380 nm. The emitted fluorescence was deflected through a 400-nm dichroic mirror and subsequently filtered at 510 nm. The signal was converted to 25 ns, 5V transistor-transistor-logic (TTL) pulses in a photomultiplier tube (PM28B; Thorn EMI). The resulting pulses were counted by a dual photon counter (Newcastle Photometrics) and recorded every second to give a ratio of emitted intensities at excitation λ^s of 340 and 380 nm, F_{340}/F_{380}.

The cytosolic Ca^{2+} measuring system was calibrated using an established protocol for intracellular calibration (Shankar et al., 1993). In brief, fura 2–loaded osteoclasts were bathed in Ca^{2+}-free, EGTA-containing solution containing 130 mM NaCl, 5 mM KCl, 5 mM glucose, 0.8 mM $MgCl_2$, 10 mM Hepes, and 0.1 mM EGTA. 5 μM ionomycin was first applied to obtain the minimum ratio due to lowest cytosolic Ca^{2+} (R_{min}) and the

maximum fluorescence intensity at 380 nm (F_{max}). 1 mM $CaCl_2$ was then applied with 5 μM ionomycin to obtain values of the maximum ratio due to an elevated cytosolic Ca^{2+} (R_{max}) and the minimum fluorescence intensity at 380 nm (F_{min}). The dissociation constant K_d for Ca^{2+} and fura 2 is 224 nM (20°C, 0.1 M, pH 6.85). The values were substituted into the equation: $[Ca^{2+}] = K_d \times [(R - R_{min})/(R_{max} - R)] \times [(F_{max}/F_{min})]$. Mean changes (Δ) in the cytosolic Ca^{2+} concentration ($[Ca^{2+}]$) were then calculated by subtracting peak from basal cytosolic $[Ca^{2+}]$. Statistical comparisons of cytosolic Δ $[Ca^{2+}]$ were made by Analysis of Variance (ANOVA) with Bonferroni's Correction for Inequality.

Bone Resorption Assay

Bone resorption was measured using the pit assay (Boyde et al., 1984; Chambers et al., 1984; Dempster et al., 1987). In brief, the bones from 24- to 48-h-old rats were sliced in 3.5 ml M199-H, and the resulting cell suspension was settled onto devitalized cortical bone slices (4 mm × 4 mm) for 30 min. After the removal of nonadherent cells by gentle rinsing, the slices were transferred to a multiwell dish containing M199-E (with 10% FBS vol/vol). Either vehicle or anti-CD38 antibody (1:500 or 1:5,000) were applied together with 1 mM NAD^+.

The slices were incubated for 24 h in humidified CO_2 (5%) (pH 6.9), after which they were fixed with glutaraldehyde (10% vol/vol) and stained for the presence of tartrate-resistant acid phosphatase (TRAP) using a kit (Kit 386A; Sigma Chemical Co.). The number of osteoclasts with two or more nuclei was determined on each slice using a light microscope (Olympus). The cells were removed by treating the slices with NaOCl (5 min), and the slices rinsed with distilled water followed by acetone, and then air-dried. The slices were stained subsequently with toluidine blue (1% vol/vol, in 1% wt/vol borate, 5 min). The number of resorption pits was determined on each slice by light microscopy. Notably, each experiment was performed with osteoclasts obtained from three animals with five or six bone slices per treatment. The number of pits or osteoclasts per bone slice was expressed as a mean ± SEM. Student's unpaired *t* test was used to analyze the effect of treatment, which was considered significant at $P < 0.05$.

Supernatant IL-6 Measurements by ELISA

Osteoclasts on coverslips were bathed in a multiwell dish containing 500 μl M199-E (with 10% FBS vol/vol) for 6 h in the presence of either vehicle or anti-CD38 antibody (1:500) and NAD^+ (1 mM). The culture medium was removed and its IL-6 level was measured with an ELISA kit (M6000; R&D). In brief, 96-well plates coated with a polyclonal anti–mouse IL-6 antiserum were used to accommodate 50 μl of assay diluent (buffered protein) and 50 μl of standard, control, or sample. After incubation (20°C, 2 h), the wells were aspirated, washed repeatedly, and loaded with 100 μl horseradish peroxidase–conjugated anti–IL-6 antibody. After a further incubation (20°C, 2 h), 100 μl of substrate solution containing H_2O_2 and tetramethylbenzidine, was added to each well. Finally, a further incubation (30 min) was followed by the addition of 100 μl of dilute HCl to stop the reaction. The optical density of each sample was measured at 450 nm on a microplate reader (BioRad). IL-6 was estimated from the standard curve in triplicate experiments and represented as mean ± SEM. Differences between control and treatment were assessed by the Student's unpaired *t* test.

Results

Isolation and DNA Sequence Analysis of a 2.8-kb Rabbit Osteoclast CD38 cDNA

To obtain full-length CD38 cDNA clones, a rabbit osteoclast cDNA library was screened. A 293-bp CD38 cDNA coding region DNA fragment was initially cloned and used as probe. A single positive cDNA clone was identified after screening 1×10^7 independent phage recombinants; this contained a 2.8-kb EcoRI-XhoI insert in the plasmid pBluescript-SK (termed SL385). The sequence of the full-length SL385 CD38 insert was obtained. Sequence analysis confirmed the presence of the CD38 coding sequence and extended into 3′-untranslated region (Fig. 1). The osteoclast CD38 cDNA sequence was 71, 69, and 66% similar to corresponding full-length CD38 cDNA sequences of mouse, rat, and human CD38 (obtained from the GenBank database) (Fig. 1). No significant homology was found, however, between the sequence of the insert and any other sequence in the GenBank database. Fig. 2 shows the predicted amino acid sequence of the full-length rabbit osteoclastic CD38. There was a 59, 59, and 50% similarity between this sequence and that of mouse, rat, and human CD38 (GenBank), respectively. The relative sequence divergence suggests that the amplified DNA product codes for a yet uncharacterized member of the CD38 family of cyclases.

CD38 mRNA in Single Osteoclasts Demonstrated by In Situ RT-bPCR Cytoimaging

CD38 mRNA expression in isolated single osteoclasts was investigated by in situ RT-PCR cytoimaging using the same primers as used for PCR cloning (above). Fig. 3 shows light micrographs of histostained osteoclasts after RT-PCR. Panel i shows an unstained osteoclast (negative controls) in an experiment in which primers were omitted from the reaction mixture. Panels ii and iii show osteoclasts in which the intense bluish-brown staining represents, respectively, mRNA expression for cathepsin K (cell-specific positive control) or GAPDH (housekeeping gene). Panels iv to vi show intense CD38 mRNA histostaining in osteoclasts that were either incubated with vehicle (iv), 10 ng/liter IL-6 (v), or 10 μg/liter IL-6 (vi).

Fig. 4 shows a semi-quantitative analysis of staining intensity using a method modified from that reported by Adebanjo et al. (1998). Osteoclasts staining for CD38 mRNA were thus assessed by a blinded observer who assigned an intensity level to the staining as a number between 0 and 4 (no staining to intense staining). Three experiments were pooled to derive frequency histograms relating the number of cells to their assigned intensity score. Osteoclasts that underwent in situ RT-PCR without added primers (control) showed a skewed distribution to the left (i, $n = 26$ cells). Cells incubated with primers, but without treatment for 6 h with IL-6 (ii, $n = 49$ cells) or those treated with 10 ng/liter IL-6 (iii, $n = 53$ cells), showed a normal (Gaussian) distribution of their assigned scores. The data became significantly skewed ($P < 0.05$) to the right when osteoclasts were treated with 10 μg/liter IL-6 (iv, $n = 29$ cells). In contrast, the expression of mRNA for GAPDH, the housekeeping gene, followed a similar distribution in all three experimental sets, namely no treatment, 10 ng/liter IL-6, and 10 μg/liter IL-6 (not shown). Taken together, the results showed that a much larger proportion of cells stained intensely with 10 μg/liter IL-6 compared with 10 ng/liter IL-6, suggesting that the former concentration of IL-6 might enhance CD38 mRNA levels. As in our earlier study (Adebanjo et al., 1998), we must emphasize that the results are semi-quantitative at best, due not only to the inherent pitfalls of the in situ RT-PCR technique, but also because the cells may undergo slight margin retraction resulting in scoring artifacts. Again, as before, we have excluded obviously retracted cells, as in these cells, staining is likely to appear more intense due to cytoplasmic condensation.

```
RABBIT:                                                    GGTGCCGCGGCTCCCTCCCCACCCCAGCCCGGCGCTCTCCTCGCCCGCTTGGCCCCGCAGAACCCGCACGGCGCGCT -1

RABBIT: ATG CCC GAC TAC GAG TTC AGC CCC GCG TCG GGG GAC AGA CCC CGC AGC TGG ATC TCT AAG CAA GTC CTG ATC GTC CTC GGC 81
MOUSE:  ATG GCT AAC TAT GAA TTT AGC CAG GTG TCT GGG GAC AGA CCT GGC TGC CGC CTC TCT AGG AAA GCC CAG ATC GGT CTC GGA 81
RAT:    ATG GCC AAC TAT GAA TTT TCC CAG GTG TCT GAG GAC AGA CCT GGC TGC CGC CTC ACT AGG AAA GCC CAG ATC GGT CTT GGA 81
HUMAN:  ATG GCC AAC TGC GAG TTC AGC CCG GTG TCC GGG GAC AAA CCC TGC TGC CGG CTC TCT AGG AGA GCC CAA CTC TGT CTT GGC 81

RABBIT: GTG TGT CTC CCG GTG ATT TTG GCC CTG GCG ATC TGG GTG GGA GTC CTG ACC TGG CGC CAG AGC TCC ATG --- --- --- --- 150
MOUSE:  GTG GGT CTC CTG GTC CTG ATC GCC TTG GTA GTA GGG ATC GTG GTC ATA CTT CTG AGG CCG CGC TCA CTC CTG GTG TGG ACT 162
RAT:    GTG GGT CTC CTG CTC CTG GTC GCC TTG GTA GTG --- GTC GTG GTC ATA GTT CTG TGG CCG CGC TCA CCC CTG GTG TGG AAA 159
HUMAN:  GTC AGT ATC CTG GTC CTG ATC CTC GTC GTG GTG CTC GCG GTG GTC GTC CCG AGG TGG CGC CAG ACG --- --- --- TGG AGC 153

RABBIT: --- --- GGC GCC ACC GAC CAC GTC TCT GCG ATC GTC CTG GGG CGA TGC CTC ACC TAC ACA CGG AAC ATG CAC CCG GAG CTG 225
MOUSE:  GGA GAG CCT ACC ACG AAG CAC TTT TCT GAC ATC TTC CTG GGA CGC TGC CTC ATC TAC ACT CAG ATC CTC CGG CCG GAG ATG 243
RAT:    GGG AAG CCT ACC ACG AAG CAC TTC GCT GAC ATC ATC TTG GGA CGC TGC CTG ATC TAT ACT CAA ATC CTC CGG CCG GAG ATG 240
HUMAN:  GGT CCG GGC ACC ACC AAG CGC TTT CCC GAG ACC GTC CTG GCG CGA TGC GTC AAG TAC ACT GAA ATT --- CAT CCT GAG ATG 231

RABBIT: AGA AAT CAG GAT TGT AAA AAA ATA CTG AAC ACC TTC ACA AGT GCA TTT GTT TCC AAG GAT CCT TGC AAC ATT ACA AAA GAA 306
MOUSE:  AGA GAT CAG AAC TGC CAG GAG ATA CTG AGT ACA TTC AAA GGA GCA TTT GTT TCC AAG AAC CCT TGC AAC ATC ACA AGA GAA 324
RAT:    AGA GAT CAG GAC TGC AAG AAG ATA CTA AGT ACA TTC AAA AGA GGG TTT ATT TCC AAG AAT CCT TGC AAC ATC ACC AAT GAA 321
HUMAN:  AGA CAT GTA GAC TGC CAA AGT GTA TGG GAT GCT TTC AAG GGT GCA TTT ATT TCA AAA CAT CCT TGC AAC ATT ACT GAA GAA 312

RABBIT: GAC TAT CAA CCA CTG ATT GAT TTG GTC ACT CAA ACT GTT CCT TGC AAC AAG ACT CTC TTT TGG AGC AGA TCA AAA GAG CTG 387
MOUSE:  GAC TAC GCC CCA CTT GTT AAA TTG GTC ACT CAA ACC ATA CCA TGT AAC AAG ACT CTC TTT TGG AGC AAA TCC AAA CAC CTG 405
RAT:    GAC TAC GCA CCA CTG GTT AAA TTG GTT ACT CAA ACC ATA CCA TGT AAC AAG ACT CTC TTT TGG AGC AAG TCC AAA CAC CTG 403
HUMAN:  GAC TAT CAG CCA CTA ATG AAG TTG GGA ACT CAG ACC GTA CCT TGC AAC AAG ATT CTT CTT TGG AGC AGA ATA AAA GAT CTG 393

RABBIT: GCC CAT CAG TAC TCA GGG ATC CAG AAA GAG ATG TTC ACT CTG GAG GAC ACG CTG CTG GGT TAC ATT GCT GAC AAC CTT GTG 468
MOUSE:  GCC CAT CAA TAT ACT TGG ATC CAG GGA AAG ATG TTC ACC CTG GAG GAC ACC CTG CTG GGC TAC ATT GCT GAT GAT CTC AGG 486
RAT:    GCC CAT CAG TAT ACT TGG ATC CAG GGG AAA ATG TTC ACC CTG GAG GAC ACA CTG CTG GGC TAT ATT GCA GAT GAT CTC AGG 483
HUMAN:  GCC CAT CAG TTC ACA CAG GTC CAG CGG GAC ATG TTC ACC CTG GAG GAC ACG CTG CTA GGC TAC CTT GCT GAT GAC CTC ACA 474

RABBIT: TGG TGT GGA GAT CCC AGA ACT TCT GAA GTG AAG GAA GAA TTT TGC CCA TAT CGG AAT GAA AAC TGC AGC AGC ACT GCT ACT 549
MOUSE:  TGG TGT GGA GAC CCT AGT ACT TCT GAT ATG AAC TAT GTC TCT TGC CCA CAT TGG AGT GAA AAC TGT CCC AAC AAC CCT ATT 567
RAT:    TGG TGT GGA GAC CCC AGT ACT TCC GAT ATG AAC TAT GAC TCT TGC CCA CAT TGG AGT GAA AAT TGT CCC AAC AAC CCT GTT 564
HUMAN:  TGG TGT GGT GAA TTC AAC ACT TCC AAA ATA AAC TAT CAA TCT TGC CCA GAC TGG AGA AAG GAC TGC AGC AAC AAC CCT GTT 555

RABBIT: TCT GTG TTC TGG ACC GTG GTT TCT CAG AAA TTT GCA GAA TCT GCC TGT GGT ACC GTC TAT GTG ATG CTC AAT GGG TCC AGA 630
MOUSE:  ACT ATG TTC TGG AAA GTG ATT TCC CAA AAG TTT GCA GAA GAT GCC TGT GGT GTG GTC CAA GTG ATG CTC AAT GGG TCC CTC 648
RAT:    GCT GTG TTC TGG AAT GTG ATT TCC CAA AAG TTT GCA GAA GAT GCC TGT GGT GTG GTC CAA GTG ATG CTC AAT GGG TCC CTC 645
HUMAN:  TCA GTA TTC TGG AAA ACG GTT TCC CGC AGG TTT GCA GAA GCT GCC TGT GAT GTG GTC CAT GTG ATG CTC AAT GGA TCC CGC 636

RABBIT: ACT ACA GCC TTT AGC AAA GCC AGC ACT TTT GGA AGT GTG GAA GTC TTC AAT TTG CAC CCA GAC AGG GTT CAT ACA CTT CAT 711
MOUSE:  CGT GAG CCG TTT TAC AAA AAC AGC ACC TTT GGA AGT TTG GAA GTC TTT AGT TTG GAC CCA AAT AAG GTT CAT AAA CTA CAG 729
RAT:    AGT GAG CCA TTT TAC AGA AAC AGC ACC TTT GGA AGT GTG GAA GTC TTT AAT TTG GAC CCA AAT AAG GTT CAT AAA CTA CAG 726
HUMAN:  AGT AAA ATC TTT GAC AAA AAC AGC ACT TTT GGG AGT GTG GAA GTC CAT AAT TTG CAA CCA GAG AAG GTT CAG ACA CTA GAG 717

RABBIT: GCC TGG GTG ATG CAT GAC ATT GGA GGA GTT GAA AGG GAC TCG TGC TTA GGT TCC TCC ATA AAG GAG TTG AAA TCG ATC GTA 792
MOUSE:  GCC TGG GTG ATG CAC GAC ATC GAA GGA GCT TCC AGT AAC GCA TGT TCA AGC TCC TCC TTA AAT GAG CTG AAG ATG ATT GTG 810
RAT:    GCC TGG GTA ATG CAT GAC ATT AAA GGA ACT TCC AGT AAT GCA TGT TCG AGC CCC TCC ATA AAT GAG CTG AAG TCG ATT GTG 807
HUMAN:  GCC TGG GTG ATA CAT GGT GGA AGA GAA GAT TCC AGA GAC TTA TGC CAG GAT CCC ACC ATA AAA GAG CTG GAA TCG ATT ATA 798

RABBIT: AAC CAG AGG AAC ATT TCC TTT TTC TGC CAG GAT GAC TAC AGG CCT GCC AGG TTT GTC CAA TGC GTG AGA CAT CCG GAG CAT 873
MOUSE:  CAG AAA AGG AAT ATG ATA TTT GCC TGC GTG GAT AAC TAC AGG CCT GCC AGG TTT CTT CAG TGT GTG AAG AAC CCT GAG CAC 891
RAT:    AAC AAA AGG AAT ATG ATA TTT GCC TGC CAG GAT AAC TAC CGA CCT GTA AGA TTT CTT CAG TGT GTG AAG AAT CCT GAG CAT 888
HUMAN:  AGC AAA AGG AAT ATT CAA TTT TCC TGC AAG AAT ATC TAC AGA CCT GAC AAG TTT CTT CAG TGT GTG AAA AAT CCT GAG GAT 879

RABBIT: CCG TCT TGC AGC GTC CTG ATG TGA GCC CAC TGC CAT GGT GCC TGG ATC TTC AGC CCC CCT GTT CAC ATC AAC ACG CAC AAC 954
MOUSE:  CCA TCG TGT AGA CTT AAT ACG TGA                                                                          915
RAT:    CCA TCA TGT AGA CTT AAT GTG TGA                                                                          912
HUMAN:  TCA TCT TGC ACA TCT GAG ATC TGA                                                                          903

RABBIT: ACCGGATGCACTGGTGCAGAGCAGATGTGAAGGAGGGTCTCCCGTCAAGATGTGAACACAGAGATGGAAATATTTTCCTTCAAAGGCTTGAAATAGTTTATGTTATT 1061
        GGCATAGCTTTTATTGTAATCTGCAGACACTCAAAAGTATTATTGTACAAATTTAGAATGAAAATTTTATATTGTTATTTCATGTTCATGTGACACTTTTATGTTGT 1168
        TTTTATGTTGGGAACATTCTTTCTATTGAGAAAAAACCATACCAAACCTTTCTTATTAGACCAGACATGGTCTATATATTTTATAGCCTTCCTACAGATGGTCAAAC 1275
        TGTAAACTCCATAGTTATGGGTTAAGTTGGGATTATCCCTTGGAAAAATTATTTTGTAGGATATTTTGTGTAGGATGTTTTACCTCTAACCCTTCCTAGAGCTCCAT 1382
        GAGCTTGGTATTATTATCTTCCATTTTTTAGATGAGAAAATGGGAGTTTAGAGCAGTTACATGATTTACATAAAGTTATCCATCTAGAATCAAGGTAGAGGCTGGAT 1489
        TCTCACAGCTGTCCATCTCTGAAGTACAGGTGCTCTCTCCTTCTAGGTCTGTGATAGACTAGATATGACAGACAGTATATATATATTTTCTCTTCCAACACATGCGT 1596
        GTAGCATTGAATTGAACACAATAGAATCTGGAATGTGATCTTTCTGGATGGCTTCATAACAAATACCTTCCCCTCCTCCTCCTTCTCTATTCCTGTTCAGTGAGTCA 1703
        TATATGTTGGTTGCACTTCAGTGGCAATTTATGCATTCTCCCTTCTTGTTTTGGATCCATCATACTTGGGACTCATATATTTTGCTACTATTTCAAAGAACTAACTT 1810
        ACAGCTCTATTGATTTTTCTTTGTATTAAATTGCTTTTTGCTCCTCTCTTTATTATTAGAAATACAAAAATTCCTTTGAGTTTCTTTGAGTATTTTTATTCAGCATC 1917
        TTGAAATGAAAGCTTGGATCACTGATTTTTCAGCCTATCTTCTTTTCTCACACATGCAGTTTAGTCTATAGATGTTTCCTGAGCTCTATATTAGCTGTAGTTCTTTA 2024
        AAAAAATGGATTTGAGAAGCAGAGAGAGATAGACATATAGATAGATAGATAGATAGATAGATATGTCTTTCATCCACTGGTTCACTCCCCAGCTGTACCCAACAGCTAGGA 2131
        CTGGCTCAGGCCAAAGCCAAGAGCCAGGACCTCAATCCAGGCCTCCCATGTGGGTGGCAGGAACCCAATTACTTGAGTCATTACCCGTTGCCCCCCAGGGTTGGCAT 2238
        TAGCAAGAAAGCTGAAGTCAGGTGCTAGAGCCAGATGTTTTGATATGTAATGTGGGTGTTTAAACCAGCGTGTTAACTACTAGTCTGAACACTCACCCTGCAGCTAC 2345
        AGCTCTAGAGTTTTATTATGTCCCTTTCATTATCATTCACTTAAAGATATTTTCTAATCTCATTGTTATTTAGAAATACATTCCTTAATTTTCAAAATTCAGACTGT 2452
        CTAGTTTTTTTAAAAGATGAACATGTTGAGCCGGCGCCGTGGCTCAATAGGCTAATCCTCCACCTTGCGGCGCCGGCACACCGGGTTCTAGTCCCGGTTGGGGCGCC 2559
        GGATTCTGTCCCGGTTGCCCCTCTTCCAGGCCAGCTCTCTGCTATGGCCAGGGAGTGCAGTGGAGGATGGCCCAGGTGCTTGGGCCCTGCACCCCATGGGAGACCAG 2666
        GAAAAGCACCTGGCTCCTGGCTCCTGCCAGGATCAGCGCGGTGCGCCGGCTGCAGCGGCGGCCATTGGAGGGTGAACCAGCGGCAAAAGGAAGACCTTTCTCTCTGT 2773
        CTCTCTCTCTCACTGTCCTCGTGCC                                                                                2798
```

Figure 1. Nucleotide sequence of rabbit osteoclast CD38 cDNA compared with the known mouse, rat, and human sequences, as shown. The respective sequences were 59, 59, and 50% homologous with the rabbit CD38 sequence. The 5′ and 3′-untranslated regions (−1 to –76 bp and 898 to 2,798 bp, respectively) are also shown. The start and stop codons are indicated in bold. Gaps are introduced to maximize homology.

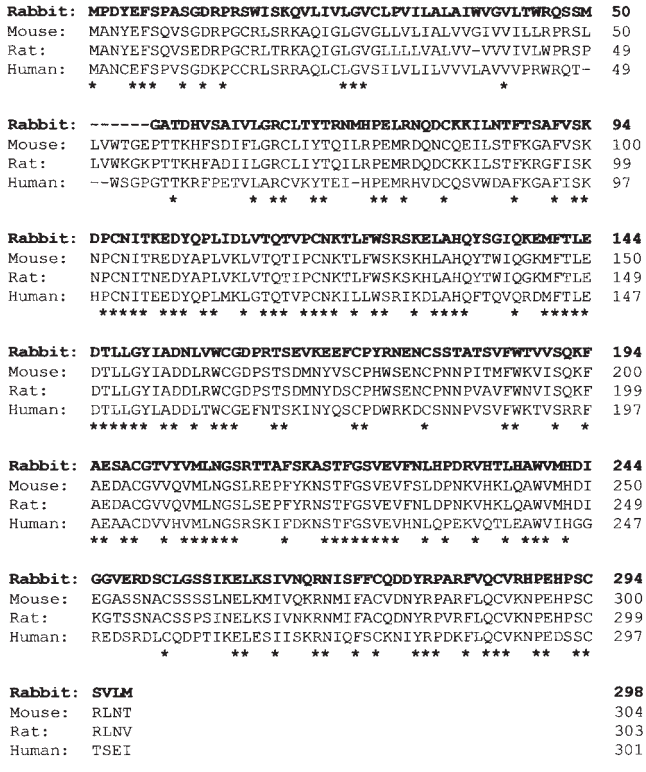

Figure 2. Predicted amino acid sequence of rabbit osteoclast CD38 compared with the known mouse, rat, and human sequences, as shown. The respective sequences were 69, 61, and 58% homologous with the rabbit CD38 sequence. Gaps are introduced to maximize homology. Asterisks indicate across-species identity of residues.

CD38 Localization to the Osteoclast Plasma Membrane

We next examined whether our highly specific anti-CD38 antibody, A10, bound to the surface of intact live osteoclasts. This agonist antibody has previously been shown to bind to, and activate, the CD38 antigen in several systems (Funaro et al., 1990). Fig. 5 (B–D) shows confocal microscopic images taken at 1-μm intervals in the coronal plane of CD38-positive osteoclasts. Intense, strictly peripheral, immunostaining was visualized distinctly reminiscent of plasma membrane staining. Notably, CD38-negative fibroblasts were found not to stain with the antibody (not shown). Also of note is that every one of the ~20 osteoclasts examined in each different experiment showed positive staining. Furthermore, all cells remained negative for trypan blue, excluding membrane damage that would otherwise permit antibody access into the cytosol.

Control experiments were performed by (a) not including the anti-CD38 antibody (not shown); (b) using preimmune mouse IgG instead of the antibody (not shown); (c) using an irrelevant anti-ryanodine receptor antibody, Ab^{34} (Fig. 5 A). That osteoclasts did not stain with any such treatment provided clear evidence for specificity. Note that Ab^{34} was raised against a cytosolic calmodulin-binding sequence of the RyR, and hence, is known not to stain the surface of nonpermeabilized osteoclasts (Zaidi et al., 1995). A negative result with the latter antibody further attests to an intact plasma membrane.

We further confirmed that the CD38 protein was present in isolated osteoclast plasma membranes by Western blotting using a different antagonist anti-CD38 antibody (Sigma Chemical Co.). A ~46 kD band was observed when plasma membranes purified by sucrose gradient centrifugation were electrophoresed and immunoblotted (Fig. 6). A further, significantly weaker, band of a smaller molecular weight (~39 kD) was also seen; this may represent a degradation product, but we are unclear of its identity. The latter band was not obvious when post-nuclear membranes from osteoblastic MC3T3-E1 cells were similarly immunoblotted. Note that the purity of the osteoclastic preparations was >99% based on TRAP staining (see Materials and Methods).

ADP Ribosyl Cyclase Activity in Osteoclast Plasma Membranes in the $NGD^+ \rightarrow$cGDPr Assay

CD38 is not only an ADP-ribosyl cyclase that converts NAD^+ to cADPr, but is also an ADP hydrolase converting active cADPr to inactive ADP-ribose. It is difficult to separate the two reactions that proceed simultaneously. We have therefore used an assay that monitors cyclization of NGD^+ to cGDPr, a nonhydrolyzable cADPr surrogate. Thus, the rate of cGDPr formation, in the absence of its breakdown, will more accurately reflect the ADP-ribosyl cyclase activity of CD38. Furthermore, cGDPr is a fluorescent compound that can be quantitated by fluorimetry. We found that osteoclast plasma membranes synthesized cGDPr at a rate of 4.3 nmoles/min/mg protein (Fig. 7). The anti-CD38 antagonist antibody (Sigma Chemical Co.) inhibited cGDPr formation significantly, thus attributing the observed ADP ribosyl cyclase activity to CD38. Enzyme activity was also inhibited significantly by addition of NAD^+ (400 μM), indicating a possible competition between the two nucleotides. Similar results were obtained from postnuclear membranes prepared MC3T3-E1 osteoblasts (not shown).

Cytosolic Ca^{2+} Signals Triggered through CD38 Activation and cADPr Generation

Having established the presence of CD38 in the osteoclast plasma membrane, we next investigated the effects of its activation by the agonist anti-CD38 antibody. Thus, we measured changes in cytosolic [Ca^{2+}] in response to application of NAD^+ (substrate) in the presence of the agonist antibody. Expectedly, only in the presence of the antibody (1:500), did 1 mM NAD^+ trigger a cytosolic [Ca^{2+}] elevation (Fig. 8 A). This result was consistent with an activated CD38/ADP-ribosyl cyclase that catalyses cADPr generation from NAD^+. In separate experiments, the anti-CD38 antibody itself, in the absence of NAD^+, did not elevate cytosolic [Ca^{2+}], indicating that the substrate, NAD^+, was necessary for CD38-induced Ca^{2+} signaling (not shown). Finally, 1 mM NAD^+ failed to trigger a cytosolic Ca^{2+} signal in the presence of the control anti-RyR antibody, Ab^{34}, further confirming response specificity.

At higher, 10 mM, NAD^+ concentrations, a marked elevation in cytosolic [Ca^{2+}] was noted even in the absence of the antibody (Fig. 8 A). This response was significantly different ($P = 0.013$) to the control response (1 mM NAD^+ alone), but did not differ significantly ($P = 0.22$)

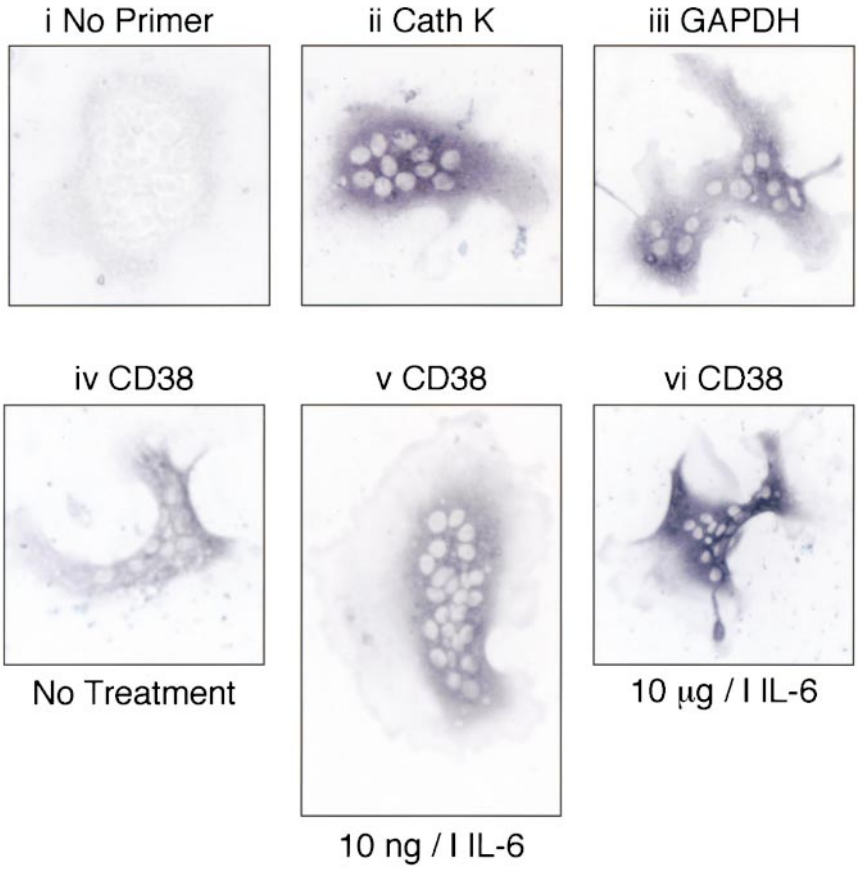

Figure 3. Histostained osteoclasts following in situ RT-PCR for detection of CD38 mRNA. i shows a negative control from a representative experiment i.e., without added primer. ii and iii represent histostaining for cathepsin K (Cath K) (cell-specific positive control) and glyceraldehyde-3-phosphate dehydrogenase (GAPDH) mRNA (housekeeping gene). Panels iv to vi show CD38 mRNA staining in osteoclasts incubated either in vehicle (iv) or with 10 ng/liter IL6 (v) or 10 μg/liter IL6 (vi). For details and primer sequences refer to Materials and Methods.

from the response triggered by 1 mM NAD^+ with antibody (Fig. 8 A).

We further demonstrated CD38-specificity of the NAD^+-induced cytosolic Ca^{2+} response by preincubating osteoclasts with the anti-CD38 antagonist antibody (Sigma Chemical Co.) before application of 10 mM NAD^+. The antagonist antibody attenuated the magnitude of the cytosolic Ca^{2+} response significantly (Fig. 8 C).

To determine whether NAD^+ triggered the release of Ca^{2+} from intracellular stores, we carried out experiments with 10 mM NAD^+ in the presence or absence of 2 mM EGTA (to chelate extracellular Ca^{2+} to near-nanomolar levels) or thapsigargin (a microsomal membrane Ca^{2+}-ATPase inhibitor that is known to deplete intracellular Ca^{2+} stores). The response to 10 mM NAD^+ in Ca^{2+}-free, EGTA-containing medium remained unchanged compared with that to 10 mM NAD^+ in 1.25 mM Ca^{2+} ($P = 0.335$). Furthermore, Fig. 8 B shows that when cells were treated with 4 μM thapsigargin, there was a significant attenuation of the cytosolic Ca^{2+} response to 10 mM NAD^+. However, it is notable that thapsigargin did not completely abolish the cytosolic Ca^{2+} response to NAD^+ suggesting that the Ca^{2+} signal was not completely dependent upon the fullness of intracellular Ca^{2+} stores. Taken together, the results suggested that NAD^+ primarily triggered the release of Ca^{2+} from intracellular Ca^{2+} stores, although Ca^{2+} influx may also play a role.

We next attempted to test the hypothesis that NAD^+-induced cADPr generation resulted in the activation of intracellular ryanodine receptors. For this, we examined whether the known cell permeant ryanodine receptor

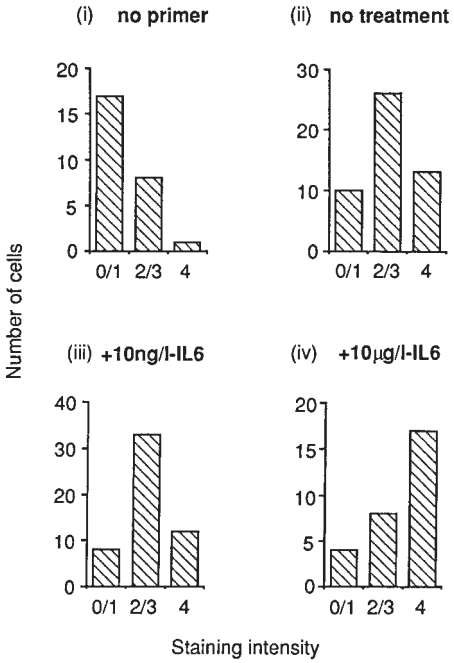

Figure 4. Semiquantitative representation in frequency histograms of intensity score after in situ RT-PCR for CD38 mRNA in osteoclasts incubated either without primer (i) or with CD38 primers without IL-6 treatment (ii) or with IL-6 treatment (10 ng/l, iii, or 10 μg/l, iv). Staining intensity was graded as described in Materials and Methods by an independent blinded observer who scored the intensity from zero (no staining) to 4 (intense staining) in three experiments. The data were analyzed statistically for skewness and shifts were considered significant if $P < 0.05$.

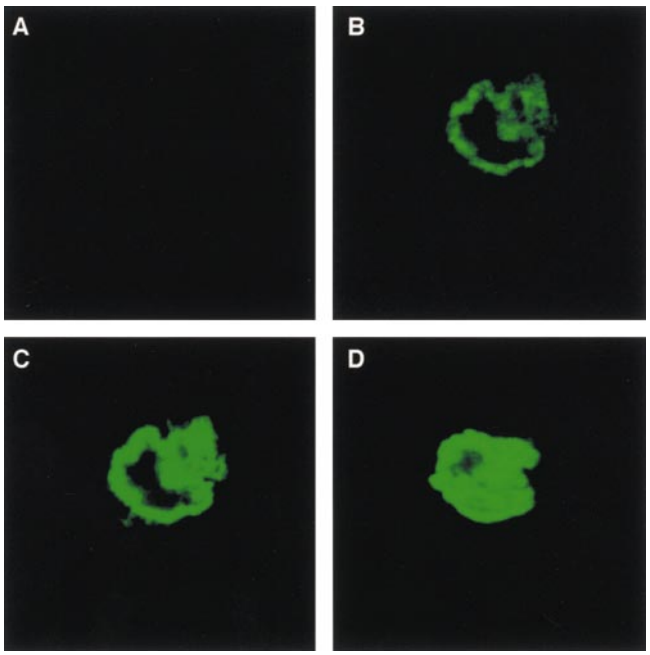

Figure 5. Confocal microscopic localization of the CD38 antigen on the osteoclast plasma membrane. Intense peripheral immunofluorescent staining of osteoclasts with a highly specific agonist anti-CD38 monoclonal antibody, A10. 1-μm-thick serial sections in the coronal plane (B–D) are shown. Note that osteoclasts incubated with no antiserum (not shown), nonimmune mouse IgG (not shown), or an irrelevant antibody (Ab^{34}) (A) do not stain. For details on confocal microscopy, see Materials and Methods.

modulators, ryanodine and caffeine, inhibited the response to applied NAD^+. Both ryanodine (5 μM) and caffeine (250 μM and 1 mM) significantly inhibited the cytosolic Ca^{2+} response to NAD^+ (*P* values, see legend to Fig. 8). Taken together, the results suggest that RyR-gated Ca^{2+} stores were being emptied in response to NAD^+, implicating, though not proving, a direct role of cADPr as a second messenger. This is consistent with our direct demonstration of cADPr-forming, ADP-ribosyl cyclase activity in the osteoclast plasma membrane as assessed by the NGD→cGDPr assay (Fig. 7). It should be emphasized that thapsigargin, ryanodine, and caffeine have all been used as tools to understand the mechanism of NAD^+-induced Ca^{2+} signaling, and in view of their other cellular actions would not be expected to reverse the effect of NAD^+ on bone resorption and IL-6 release.

Inhibition of Bone Resorption and Enhancement of IL-6 Release by CD38 Activation

We have shown that while a cytosolic Ca^{2+} change triggers resorption inhibition, it elevates IL-6 synthesis and release (Zaidi et al., 1989, Moonga et al., 1990, Adebanjo et al., 1998). Our goal, therefore, was to examine the effect of CD38 activation by NAD^+ (in the presence of its agonist antibody, A10) on bone resorption and IL-6 release. In the presence of A10, at either dilutions (1:5,000 or 1:500), 1 mM NAD^+ inhibited osteoclastic bone resorption significantly ($P = 0.034$ and $P = 0.025$, respectively, compared with vehicle-treated cells) (Fig. 9 a). Expectedly, osteoclast number per slice did not change significantly ($P > 0.05$ for either antibody dilution) (Fig. 9 b), excluding an effect of the antibody on osteoclast formation or demise. In separate experiments, the 1 mM NAD^+ (in the presence of A10, 1:500), caused a dramatic and highly significant threefold elevation ($P < 0.001$) of IL-6 release (Fig. 9 c). Taken together, the results appear consistent with the paradoxical effects of Ca^{2+} on bone resorption and IL-6 release (Moonga et al., 1990; Adebanjo et al., 1998).

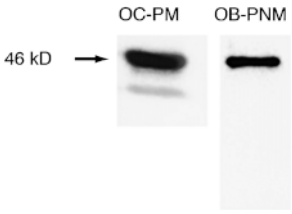

Figure 6. Western blotting after SDS-PAGE of osteoclast plasma membranes (OC-PM) (30 μg protein) and osteoblast postnuclear membranes (OB-PNM) (50 μg protein) using an antagonist anti-CD38 antibody (Sigma Chemical Co.). We identified 46-kD bands with an additional lower molecular weight band in OC-PMs. The osteoclast preparations were >99% pure as assessed by TRAP staining (see Materials and Methods).

Discussion

The multifunctional ectoenzyme, CD38, is known to modulate lymphocyte functions as critical as adhesion, proliferation and cytokine production (Cesano et al., 1998, Ferrero and Malavasi, 1997). It also functions as a counter-receptor for CD31, presumably facilitating cell-to-cell communication (Deaglio et al., 1998; Horenstein et al., 1998). It is also an ADP-ribosyl cyclase that catalyzes the formation of cADPr from NAD^+. Several reports have suggested that the latter is a cellular second messenger, somewhat akin to IP_3 (for review: Lee, 1996; Guse et al., 1999). We show that CD38 regulates osteoclastic bone resorption via the production of cADPr. Specifically, we show that a novel CD38 homologue is located in the rabbit osteoclast plasma membrane; that it possesses ADP-ribosyl cyclase activity; that its activation results in cytosolic Ca^{2+} elevation through ryanodine receptor activation; and that the cytosolic Ca^{2+} change is accompanied, quite expectedly, by an elevation in IL-6 release and resorption inhibition.

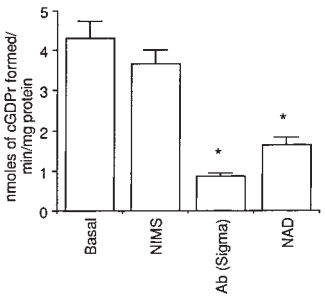

Figure 7. ADP-ribosyl cyclase activity of CD38 in isolated osteoclast plasma membranes. The conversion of the NAD^+ surrogate, NGD^+, to the nonhydrolyzable fluorescent product, cyclic GDP-ribose (cGDPr) was assessed fluorimetrically (see Materials and Methods for details). Results are expressed as a mean (± SEM) cGDPr formed in nmoles/min/mg isolated plasma membrane protein without treatment (basal) or in the presence of nonimmune mouse serum (IgG5) (NIMS), an antagonist anti-CD38 antibody (Ab; Sigma Chemical Co., 1:500) or NAD^+ (400 μM). The asterisks represent significant differences compared with basal ($P < 0.05$).

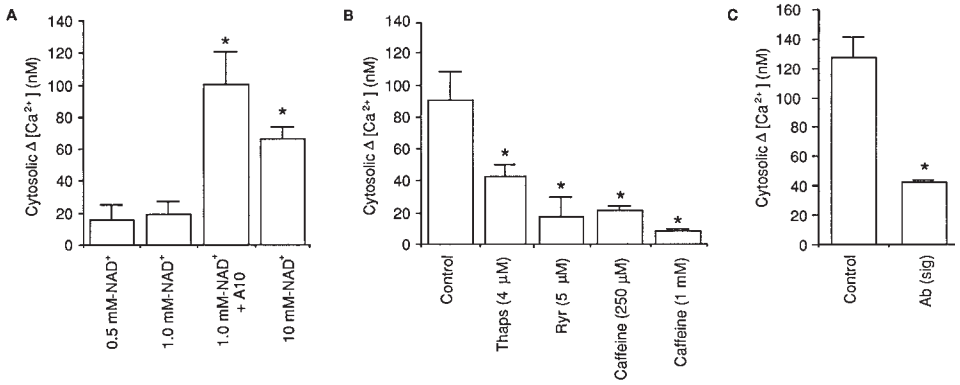

Figure 8. Effect of NAD^+ (NAD^+, concentrations as shown) on the mean change (Δ) in cytosolic [Ca^{2+}] (nM) in fura 2–loaded single osteoclasts under various experimental conditions. (A) Osteoclasts were preincubated with either vehicle or the anti-CD38 agonist antibody, A10 (1:500) in Medium 199-Hanks ([Ca^{2+}] = 1.25 mM). (B) Osteoclasts were pretreated for several min with the microsomal membrane Ca^{2+}-ATPase inhibitor, thapsigargin (4 μM), or with the cell-permeant ryanodine receptor modulators, ryanodine (4 μM) or caffeine (4 μM). (C) Osteoclasts were pretreated for 15 min with the antagonist antibody (Sigma Chemical Co.) (1:500) (Sig). Cytosolic Δ [Ca^{2+}] was calculated in each case by subtracting the basal from peak cytosolic [Ca^{2+}]. Asterisks indicate $P < 0.05$ ($n = 6$ per group).

CD38 catalyzes the cyclization of NAD^+ not only to cADPr (Howard et al., 1993), but also to the more recently described, dimeric ADPr (DeFlora et al., 1997a). While the classical action of cADPr is to release Ca^{2+} from RyR-bearing Ca^{2+} stores, dimeric ADPr potentiates this effect (DeFlora et al., 1997a). In the osteoclast, we have shown that cADPr triggers both Ca^{2+} release and Ca^{2+} influx through its action, respectively, on microsomal membrane RyRs and a uniquely positioned surface RyR-2 (Zaidi et al., 1995; Adebanjo et al., 1996). Apart from being activated by cADPr, the uniquely positioned osteoclast surface RyR-2 appears also to sense changes in the cell's ambient Ca^{2+} concentration during resorption (Zaidi et al., 1995). Any rise in cytosolic Ca^{2+} in the osteoclast triggers rapid cell retraction, diminished enzyme release, and reduced acid secretion, culminating finally, in the inhibition of bone resorption (Malgaroli et al., 1989; Zaidi et al., 1989; Datta et al., 1990; Miyauchi et al., 1990; Moonga et al., 1990). However, an increased cytosolic Ca^{2+} also enhances IL-6 secretion, possibly to release an osteoclast from the resorption inhibition induced by a high Ca^{2+} (Adebanjo et al., 1998).

The observed effect of CD38 activation in inhibiting bone resorption and elevating IL-6 release thus mirrors that of Ca^{2+}. Notably, both agents act by elevating cytosolic Ca^{2+}. Interestingly, however, cADPr-induced Ca^{2+} release also mediates the effect of CD38 in inducing other cytokines, including IL-6, interferon-γ, granulocyte-macrophage colony stimulating factor (GM-CSF), and IL-10 (Ausiello et al., 1996). Cyclic ADPr also promotes secretion of hormones, such as insulin from pancreatic β cells, and cytokines from T cells (Takasawa et al., 1998; Cesano et al., 1998). Nevertheless, it is unclear as to how these released cytokines, in turn, affect CD38 expression and cADPr formation. We provide new evidence that IL-6 enhances the expression of CD38 mRNA. This appears consistent with a NF-IL-6 site in the CD38 gene promoter (Kishimoto et al., 1998). Our in situ RT-PCR results, however, must be treated with caution in view of the known technological pitfalls and possible artifacts, which we have tried to avoid.

The Ca^{2+}-like effects of CD38 might also be relevant physiologically in the metabolic control of bone resorption via NAD^+. It is noteworthy that the energy requirement of a resorbing osteoclast is high due to its active secretion of acid and enzymes and its intense motile activity. It is therefore possible that large amounts of NAD^+ are being generated intracellularly during resorption. Significant amounts of this NAD^+ may indeed extrude from the osteoclast. Indeed, Zocchi et al. (1999) have demonstrated the existence of a saturable and bidirectional NAD^+ transport system in a variety of eukaryotic cells; the same could be true for osteoclasts. Alternatively, neighboring cells undergoing apoptosis may release much NAD^+ (Mehta et al., 1996). The extracellularly located catalytic domain of the CD38/ADP-ribosyl cyclase could then sense the NAD^+, and by catalyzing its conversion to cADPr, limit further osteoclastic resorption. Franco et al. (1998) have demon-

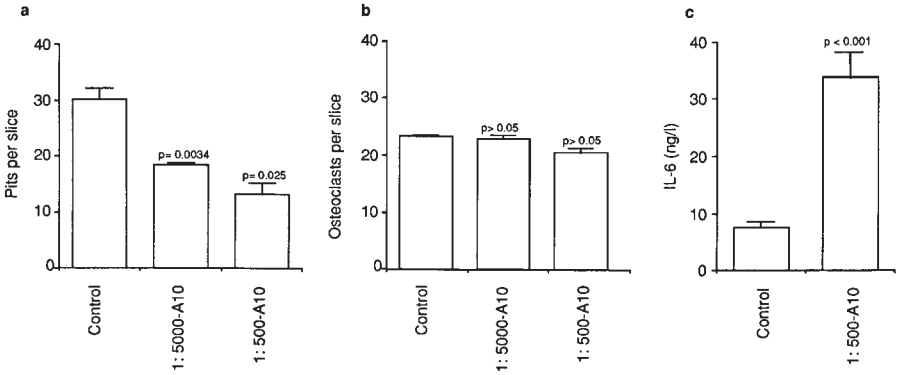

Figure 9. Effect of the agonist anti-CD38 antibody (A10, 1:5,000 or 1:500) in the presence of substrate (1 mM NAD^+) on bone resorption (a, pits per slice) and osteoclast number (b, osteoclasts per slice) as assessed in the pit assay, as well as on supernatant interleukin-6 (IL-6, ng/liter) levels (c) measured by ELISA. *P* values as indicated ($n = 10$ slices per group).

strated a role of CD38 in NAD^+ sensing in HeLa cells and human erythrocytes.

Our evidence for the production of cADPr through NAD^+ catalysis by CD38 is twofold. First, we have directly demonstrated that osteoclast plasma membranes that are positive for CD38 immunoreactivity contain ADP-ribosyl cyclase activity. This has been assessed using an assay that allows for the catalytic conversion of the NAD^+ surrogate, NGD^+, to its nonhydrolyzable and fluorescent derivative, cGDPr. We showed that the observed ADP-ribosyl cyclase activity could be inhibited noncompetitively by an antagonist antibody to CD38, confirming directly, a role for CD38 in cGDPr formation. That NAD^+ also significantly inhibited NGD^+ catalysis confirmed further that the two molecules most likely shared the same substrate-binding site. cGDPr formation in osteoclast plasma membranes thus appears truly reflective of the ADP-ribosyl cyclase activity of CD38. Second, and in line with the above, we have shown that NAD^+ application to osteoclasts triggers cytosolic Ca^{2+} release mostly from intracellular stores that are sensitive to inhibition by RyR modulators, ryanodine and caffeine. This, albeit indirect, demonstration for a role of RyRs in NAD^+-induced Ca^{2+} release further suggests a second messenger role for the generated cADPr.

Despite our molecular and biochemical demonstration of functionally active CD38/ADP ribosyl cyclase in the osteoclast plasma membrane, it remains unclear how any cADPr synthesized extracellularly could act on intracellular RyRs. Two explanations have been offered in other models (Lund et al., 1998). First, the CD38 catalytic compartment may become internalized after its recognition of substrate, thus generating cADPr intracellularly (Funaro et al., 1998; Zocchi et al., 1998, 1999). In fact, Zocchi et al. (1999) have shown, using endocytic vesicles, that NAD^+ first internalizes through a saturable transport system independent of CD38, and once, within the vesicle, is catalyzed to cADPr. The latter is then pumped out into the cytosol to affect Ca^{2+} release from RyR-gated Ca^{2+} stores. It has been suggested that agonist antibodies, such as A10, may aid such internalization (Funaro et al., 1998). Indeed, A10 is known to enhance the activation and proliferation of B and T lymphocytes through enhanced cADPr production (hence the term, agonist) (Funaro et al., 1990). Such a mechanism provides one likely explanation for the synergistic effects of the A10 and NAD^+ on cytosolic Ca^{2+}. An alternative possibility, however, also exists. This is that cADPr is first generated extracellularly, and then traverses the cell membrane to interact with intracellular RyRs. Effects of extracellularly applied cADPr on cellular function have been described in rat cerebellar cells (De-Flora et al., 1996, 1997b), murine B lymphocytes (Howard et al., 1993) and rat osteoclasts (Adebanjo et al., 1996). Franco et al. (1998) have shown, however, using human erythrocyte membranes and CD38-reconstituted proteoliposomes that CD38 is a selective transporter of catalytically generated, but not exogenously added cADPr. Indeed, CD38 internalization is currently the favored hypothesis and could explain our results fully. However, the major goal of this study has not been to probe this mechanism; instead, it has been to identify a plausible role of CD38/ADP ribosyl cyclase in the control of osteoclastic bone resorption.

We have provided evidence that the NAD^+-induced Ca^{2+} signal is made up of two components, Ca^{2+} release from RyR-gated intracellular stores, and Ca^{2+} influx possibly through the uniquely positioned plasma membrane RyR-2. The role of ryanodine receptors has been generally confirmed through experiments demonstrating that the cytosolic Ca^{2+} response to NAD^+ is inhibited strongly by both ryanodine and caffeine (Fig. 8). However, these experiments have not allowed us to determine whether the respective modulators block the intracellular RyRs, or the surface RyR-2, or both. Nonetheless, we show here that the NAD^+-induced cytosolic Ca^{2+} response is maintained in Ca^{2+}-free, EGTA-containing medium, suggesting its dependence on intracellular Ca^{2+} release. Our experiments with thapsigargin, a microsomal membrane Ca^{2+}-ATPase inhibitor known to deplete intracellular Ca^{2+} stores, appear more conclusive. These results show that thapsigargin attenuates, but does not abolish the cytosolic Ca^{2+} signal, suggesting that there is a component of extracellular Ca^{2+} influx. This, however, remains to be established.

In conclusion, we have documented a new function for osteoclastic CD38. We believe that its activation at the osteoclast plasma membrane results in cytosolic Ca^{2+} release from RyR gated intracellular Ca^{2+} stores via cADPr generation from NAD^+. The released Ca^{2+} then signals a reduction in bone resorption and a paradoxical elevation of IL-6 release. It is therefore possible that the CD38/Ca^{2+}/IL-6 pathway may have a critical role in coupling an osteoclast's metabolic activity with its resorptive function. Our current studies with CD38−/− mice should shed more light on the function of CD38 in osteoclast control (Kato et al., 1999).

The authors are grateful to Professor Iain MacIntyre (William Harvey Research Institute, London, UK) for his encouragement and support; Christopher L.-H. Huang (Physiological Laboratory, Cambridge, UK) for helpful discussion; Qinwu Lin (Wistar Institute, Philadelphia, PA) for assistance with confocal microscopy; Jerry Rosenzweig (Geriatrics Department, Veterans Affairs Medical Center, Philadelphia, PA) for assistance in grant management; and Stacey Marshall (University of Pennsylvania, Philadelphia, PA) for illustrations.

M. Zaidi acknowledges the support of the National Institutes of Health (RO1-AG14702-01) and the Department of Veteran's Affairs.

Submitted: 8 October 1998
Revised: 14 July 1999
Accepted: 26 July 1999

References

Adebanjo, O.A., V.S. Shankar, M. Pazianas, A. Zaidi, C.L.-H. Huang, and M. Zaidi. 1994. Modulation of the osteoclast Ca^{2+} receptor by extracellular protons. Possible linkage between Ca^{2+} sensing and extracellular acidification. *Biochem. Biophys. Res. Commun.* 194:742–747.

Adebanjo, O.A., V.S. Shankar, M. Pazianas, B.J. Simon, F.A. Lai, C.L.-H. Huang, and M. Zaidi. 1996. Extracellularly applied ruthenium red and cADP ribose elevate cytosolic Ca^{2+} in isolated rat osteoclasts. *Am. J. Physiol.* 270:F469–F475.

Adebanjo, O.A., B.S. Moonga, T. Yamate, L. Sun, C. Minkin, E. Abe, and M. Zaidi. 1998. Mode of action of interleukin-6 on mature osteoclasts. Novel interactions with extracellular Ca^{2+} sensing in the regulation of osteoclastic bone resorption. *J. Cell Biol.* 142:1347–1356.

Ausiello, C.M., A.L. Sala, C. Ramoni, F. Urbani, A. Funaro, and F. Malavasi. 1996. Secretion of IFN-γ, IL-6, granulocyte-macrophage colony-stimulating factor and IL-10 cytokines after activation of human purified T lymphocytes upon CD38 ligation. *Cell. Immunol.* 173:192–197.

Berthelier, V., J.M. Tixier, H. MuHer-Steffner, F. Schuber, P. Deterre. 1998. Human CD38 is an authentic NAD(P)+ glycohydrolase. *Biochem. J.* 330: 1383–1390.

Boyde, A., N.N. Ali, and S.J. Jones. 1984. Resorption of dentine by isolated os-

teoclasts *in vitro*. *Brit. Dental J.* 156:216–220.
Cesano, A., S. Visonneau, S. Deaglio, F. Malavasi, and D. Santoli. 1998. Role of CD38 and its ligand in the regulation of MHC-nonrestricted cytotoxic T cells. *J. Immunol.* 160:1106–1115.
Chambers, T.J., O.A. Revell, K. Fuller, and N.A. Athanasou. 1984. Resorption of bone by isolated rabbit osteoclasts. *J. Cell Sci.* 66:383–399.
Datta, H.K., I. MacIntyre, and M. Zaidi. 1990. The effect of extracellular calcium elevation on morphology and function of isolated rat osteoclasts. *Biosci. Rep.* 9:747–751.
Deaglio, S., M. Morra, R. Mallone, C.M. Ausiello, E. Prager, G. Garbarino, U. Dianzani, H. Stockinger, and F. Malavasi. 1998. Human CD38 (ADP-ribosyl cyclase) is a counter-receptor of CD31, an Ig superfamily member. *J. Immunol.* 160:395–402.
De Flora, A., L. Guida, L. Franco, E. Zocchi, M. Pestarino, C. Usai, C. Marchetti, E. Fedele, G. Fontana, and M. Raiteri. 1996. Ectocellular in vitro and in vivo metabolism of cADP-ribose in cerebellum. *Biochem. J.* 320:665–671.
De Flora, A., L. Guida, L. Franco, E. Zocchi, S. Bruzzone, U. Benatti, and G. Damonte. 1997a. CD38 and ADP-ribosyl cyclase catalyze the synthesis of a dimeric ADP-ribose that potentiates the calcium-mobilizing activity of cyclic ADP-ribose. *J. Biol. Chem.* 272:12945–12951.
De Flora, A., L. Guida, L. Franco, and E. Zocchi. 1997b. The CD38/cyclic ADP-ribose system: a topological paradox. *Int. J. Biochem. Cell Biol.* 29: 1149–1166.
De Flora, A., L. Franco, L. Guida, S. Bruzzone, and E. Zocchi. 1998. Ectocellular CD38–catalyzed synthesis and intracellular Ca(2+)-mobilizing activity of cyclic ADP-ribose. *Cell Biochem. Biophys.* 28:45–62.
Dempster, D.W., R.J. Murrills, W.R. Horbert, and T.R. Arnett. 1987. Biological activity of chicken calcitonin: effects on neonatal rat and embryonic chick osteoclasts. *J. Bone Min. Res.* 2:443–448.
Fernandez, J.E., S. Deaglio, D. Donati, I.S. Beusan, F. Corno, A. Aranega, M. Forni, B. Falini, and F. Malavasi. 1998. Analysis of the distribution of human CD38 and of its ligand CD31 in normal tissues. *J. Biol. Regul. Homeost.* 12: 81–91.
Ferrero, E., and F. Malavasi. 1997. Human CD38, a leukocyte receptor and ectoenzyme, is a member of a novel eukaryotic gene family of nicotinamide adenine dinucleotide$^+$-converting enzymes: extensive structural homology with the genes for murine bone marrow stromal cell antigen 1 and aplysian ADP-ribosyl cyclase. *J. Immunol.* 159:3858–3865.
Franco, L., L. Guida, S. Bruzzone, E. Zocchi, C. Usai, and A. DeFlora. 1998. The transmembrane glycoprotein CD38 is a catalytically active transporter responsible for generation and influx of the second messenger cyclic ADP-ribose across membranes. *FASEB J.* 12:1507–1520.
Furano, A., G.C. Spagnoli, C.M. Ausiello, M. Alessio, S. Rogerro, D. Delia, M. Zaccolo, and F. Malavasi. 1990. Involvement of the multilineage CD38 molecule in a unique pathway of cell activation and proliferation. *J. Immunol.* 145:2390–2396.
Funaro, A., M. Reinis, O. Trubiani, S. Santi, R. Di Primio, and F. Malavasi. 1998. CD38 functions are regulated through an internalization step. *J. Immunol.* 160:2238–2247.
Guse, A.H., C.P. da Silva, I. Berg, A.L. Skapenko, K. Weber, P. Heyer, M. Hohenegger, G.A. Ashamu, H. Schulze-Koops, B.V. Potter, and G.W. Mayr. 1999. Regulation of calcium signalling in T lymphocytes by the second messenger cyclic ADP-ribose. *Nature.* 398:70–73.
Harada, N., L. Santos-Argumedo, R. Chang, J.C. Grimaldi, F.E. Lund, C.I. Brannan, N.G. Copeland, N.A. Jenkins, A.W. Heath, R.M.E. Parkhouse, and M. Howard. 1993. Expression cloning of a cDNA encoding a novel murine B cell activation marker. *J. Immunol.* 151:3111–3118.
Horenstein, A.L., H. Stockingert, B.A. Imhoft, and F. Malavasi. 1998. CD38 binding to human myeloid cells is mediated by mouse and human CD38. *Biochem. J.* 330:1129–1135.
Howard, M., J.C. Grimaldi, J.F. Bazan, F.E. Lund, L. Santos-Argumedo, R.M.E. Parkhouse, T.F. Walseth, and H.C. Lee. 1993. Formation and hydrolysis of cyclic ADP-ribose catalyzed by lymphocyte antigen CD38. *Science.* 262:1056–1059.
Kakudo, S., K. Miyazawa, H. Kameda, H. Mano, Y. Mori, T. Yuasa, I. Nakamura, M. Shiokawa, K. Nagahirsa, S. Tokunaga, et al. 1996 Isolation of highly enriched rabbit osteoclasts from collagen gels: a new assay system for bone resorbing activity of mature osteoclasts. *J. Bone Min. Metab.* 14:129–136.
Kameda, T., H. Mano, T. Yuasa, Y. Mori, K. Miyazawa, M. Shiokawa, Y. Nakamura, E. Hiroi, K. Hiura, A. Kameda, et al. 1997. Estrogen inhibits bone resorption by directly inducing apoptosis of bone resorbing osteoclasts. *J. Exp. Med.* 186:489–495.
Kameda, T., H. Mano, Y. Yamada, H. Takai, N. Amizuka, M. Kobori, N. Izumi, H. Kawashima, H. Ozawa, K. Ikeda, et al. 1998. Calcium-sensing receptor in mature osteoclasts, which are bone resorbing cells. *Biochem. Biophys. Res. Commun.* 245:419–422.
Kato, I., Y. Yamamoto, M. Fujimura, N. Noguchi, S. Takasawa, and H. Okamoto. 1999. CD38 disruption impairs glucose-induced increases in cyclic ADP-ribose, [Ca^{2+}]i, and insulin secretion. *J. Biol. Chem.* 274:1869–1872.
Kishimoto, H., S. Hoshino, M. Ohori, K. Kontani, H. Nishina, M. Suzawa, S. Kato, and T. Katada. 1998. Molecular mechanism of human CD38 gene expression by retinoic acid. *J. Biol. Chem.* 273:15429–15434.
Lee, H.C. 1996. Modulator and messenger functions of cyclic ADP-ribose in calcium signaling. *Recent. Prog. Horm. Res.* 51:355–388; discussion 389.
Lee, H.C., A. Galione, and T.F. Walseth. 1994. Cyclic ADP-ribose: metabolism and calcium mobilization function. *Vit. Horm.* 48:199–258.
Lee, H.C., R.M. Graeff, and T.F. Walseth. 1997. ADP-ribosyl cyclase and CD38. Multi-functional enzymes in Ca^{+2} signaling. *Adv. Exp. Med. Biol.* 419:411–419.
Lin, S.-C., T. Yamate, V.Z.C. Borba, G. Girasole, C.A. O'Brien, T. Bellido, E. Abe, and S.C. Manolagas. 1997. Regulation of the gp80 and gp130 subunits of the IL-6 receptor by sex steroids in the murine bone marrow. *J. Clin. Invest.* 100:1980–1990.
Lund, F.E., D.A. Cockayne, T.D. Randall, N. Solvason, F. Schuber, and M.C. Howard. 1998. CD38: a new paradigm in lymphocyte activation and signal transduction. *Immunol. Rev.* 161:79–93.
Malavasi, F., F. Caligaris-Cappio, P. Dellabona, P. Richiardi, and A.O. Carbonara. 1984. Characterization of a murine monoclonal antibody specific for human early lymphohemopoietic cells. *Hum. Immunol.* 9:9.
Malavasi, F., G. Bellone, L. Matera, E. Ferrero, A. Funaro, S. DeMaria, F. Caligaris-Cappio, G. Camussi, and P. Dellabona. 1985. Murine monoclonal antibodies as probes for the phenotypical, functional and molecular analysis of a discrete peripheral blood lymphocyte population exerting natural killer activity *in vitro*. *Hum. Immunol.* 14:87.
Malavasi, F., A. Funaro, M. Allesio, L.B. DeMonte, C.M. Ausiello, U. Dianzani, F. Lanza, E. Magrini, M. Momo, and S. Roggero. 1992. CD38: a multilineage cell activation molecule with a split personality. *Int. J. Clin. Lab. Res.* 22:73–80.
Malgaroli, A., J. Meldolesi, A. Zabonin-Zallone, and A. Teti. 1989. Control of cytosolic free calcium in rat and chicken osteoclasts. *J. Biol. Chem.* 264: 14342–14347.
Mehta, M., U. Shahid, and F Malavasi. 1996. Human CD38, a cell surface protein with multiple functions. *FASEB J.* 10:1408–1417.
Miyauchi, A., K.A. Hruska, E.M. Greenfield, R. Duncan, J. Alvarez, R. Barattolo, S. Colluci, A. Zambonin-Zallone, S.L. Teitelbaum, and A. Teti. 1990. Osteoclast cytosolic calcium, regulated by voltage-gated calcium channels, extracellular calcium, controls podosome assembly and bone resorption. *J. Cell Biol.* 111:2543–2552.
Moonga, B.S., D.W. Moss, A. Patchell, and M. Zaidi. 1990. Intracellular regulation of enzyme secretion from rat osteoclasts and evidence for a functional role in bone resorption. *J. Physiol. Lond.* 42:29–45.
Sambrook, J., E.F. Fritsch, and T. Maniatis. 1989. Molecular Cloning. A Laboratory Manual. Cold Spring Harbor Laboratory Press, Cold Spring Harbor, NY.
Shankar, V.S., C.M.R. Bax, B.E. Bax, A.S.M.T. Alam, B. Simon, M. Pazianas, B.S. Moonga, C.L.-H. Huang, and M. Zaidi. 1992. Activation of the Ca^{2+} "receptor" on the osteoclast by Ni^{2+} elicits cytosolic Ca^{2+} signals: evidence for receptor activation and inactivation, intracellular Ca^{2+} redistribution and divalent cation modulation. *J. Cell. Physiol.* 155:120–129.
Shankar, V.S, C.L.-H. Huang, O.A. Adebanjo, B.J. Simon, A.S.M.T. Alam, B.S. Moonga, M. Pazianas, R.H. Scott, and M. Zaidi. 1995. The effect of membrane potential on surface Ca^{2+} receptor activation in rat osteoclasts. *J. Cell. Physiol.* 162:1–8.
Shubinski, G., and M. Schlesinger. 1997. The CD38 lymphocyte differentiation marker: new insight into its ectoenzyme activity and its role as a signal transducer. *Immunity.* 7:315–324.
Takasawa, S., T. Akiyama, K. Nata, M. Kuroki, A. Tohgo, N. Noguchi, S. Kobayashi, I. Kato, T. Katada, and H. Okamoto. 1998. Cyclic ADP-ribose and inositol 1,4,5–trisphosphate as alternate second messengers for intracellular Ca^{2+} mobilization in normal and diabetic beta-cells. *J. Biol. Chem.* 273: 2497–2500.
Tezuka, K., T. Sato, H. Kamioka, P.J. Nijweide, K. Tanaka, T. Matsuo, M. Ohta, N. Kurihara, Y. Hakeda, and M. Kumegawa. 1992. Identification of osteopontin in isolated rabbit osteoclasts. *Biochem. Biophys. Res. Commun.* 186:911–917.
Zaidi, M., H.K. Datta, A. Patchell, B.S. Moonga, and I. MacIntyre. 1989. "Calcium-activated" intracellular calcium elevation: a novel mechanism of osteoclast regulation. *Biochem. Biophys. Res. Commun.* 163:1461–1465.
Zaidi, M., A.S.M.T. Alam, V.S. Shankar, B.E. Bax, B.S. Moonga, P.J.R. Bevis, M. Pazianas, and C.L.-H. Huang. 1992. A quantitative description of components of *in vitro* morphometric change in the rat osteoclast model: relationships with cellular function. *Eur. Biophys. J.* 21:349–355.
Zaidi, M., A.S.M.T. Alam, V.S. Shankar, B.E. Bax, C.M.R. Bax, B.S. Moonga, P.J.R. Bevis, C. Stevens, D.R. Blake, M. Pazianas, and C.L.-H. Huang. 1993. Cellular biology of bone resorption. *Biol. Rev.* 68:197–264.
Zaidi, M., V.S. Shankar, R. Tunwell, O.A. Adebanjo, J. MacKrill, M. Pazianas, D. O'Connell, B.J. Simon, B.R. Rifkin, A.R. Ventikaraman, et al. 1995. A ryanodine receptor-like molecule expressed in the osteoclast plasma membrane functions in extracellular Ca^{2+} sensing. *J. Clin. Invest.* 96:1582–1590.
Zaidi, M., V.S. Shankar, O.A. Adebanjo, F.A. Lai, M. Pazianas, G. Sunavala, A.I. Spielman, and B.R. Rifkin. 1996. Regulation of extracellular calcium sensing in rat osteoclasts by femtomolar calcitonin concentrations. *Am. J. Physiol.* 271:F637–F644.
Zocchi, E., L. Franco, L. Guida, D. Piccini, C. Tacchetti, and A. De Flora. 1996. NAD+ dependent internalization of the transmembrane glycoprotein CD38 in human Namalwa B cells. *FEBS. Lett.* 396:327–332.
Zocchi, E., A. Daga, C. Usai, L. Franco, L. Guida, S. Bruzzone, A. Costa, C. Marchetti, and A. De Flora. 1998. Expression of CD38 increases intracellular calcium concentration and reduces doubling time in HeLa and 3T3 cells. *J. Biol. Chem.* 273:8017–8024.
Zocchi, E., C. Usai, L. Guida, L. Franco, S. Bruzzone, M. Passalacqua, and A. De Flora. 1999. Ligand-induced internalization of CD38 results in intracellular Ca^{2+} mobilization: role of NAD transport across cell membranes. *FASEB J.* 13:273–283.